Automated lithology extraction from core photographs

Angeleena Thomas,[1*] Malcolm Rider,[1] Andrew Curtis[1] and Alasdair MacArthur propose a novel approach to lithology classification from core photographs based on object-based image analysis, an advanced method used in remote sensing and medical imaging.

Lithologies or rock types within any reservoir formation can be inferred from a combination of surface geophysical and well log data. However the ground truth is reflected in extracted core which must be examined manually by an expert geologist for lithological classification. This is a highly laborious and time consuming process. Also, large sections of core are not easily portable, and cannot be distributed in their entirety to more than one place at once. The core also inevitably deteriorates with age either naturally or by excessive handling and sampling (Blackbourn, 1990). Cores are usually stored in some remote core store where warehousing is cheap, and visits are therefore made only in cases of special need.

As a result 3D x-ray core scanning and core slab photographing are becoming more and more commonplace leading to the availability of high quality digital data of the core. This information about the subsurface is mobile, can be distributed freely, and does not deteriorate with age. These digital data can be copied and are accessible at any time according to demand.

Lithological classification can also now be carried out based on the colour and texture patterns of these high quality digital images. However, this approach requires dealing with a large amount of raw, digital data. Therefore automated classification, which can complement the skills of reservoir characterization professionals engaged in interpreting core photographs, will be a significant advance.

An object-based image analysis (OBIA) methodology is proposed for automated lithology extraction from core photographs. The proposed method contains three main steps:

1) Image segmentation, where adjacent, similar image pixels in the core photograph are grouped together as image objects (based on some predefined parameters). These act as the basic units for core photograph classification.
2) Knowledge-base design, which is entirely field dependent, where we define classes present in the field, selecting a classifier (a classification algorithm which will evaluate the likelihood that each image object belongs to each of the classes defined), and training the classifier with appropriate samples and object features that are typical of, and hence define or distinguish each class.
3) Use the trained classifier to do automated classification of the entire core photograph or other core photographs from similar geological settings.

The expert knowledge encoded within the classifier in the second step ensures accuracy in the classification method as classes are defined and appropriate training samples are selected according to current knowledge of the field heterogeneity. Also this flexible method for an expert to inject knowledge allows the method to be adapted easily to other geological settings (with appropriate modifications to suit the new field).

The proposed methodology has now been tested and verified on two core photograph intervals. The accuracy of the automated classification is assessed by comparing it to a geologist's qualitative interpretation of the same core photograph intervals.

Methodology

Data selection

The aim is to facilitate rapid automated classification of core photographs from the entire well. To start with, a small representative interval of the core photograph is taken and a classifier is trained to distinguish different lithology classes based on their textural and spectral characteristics. The trained and tested classifier can be used to obtain an automated classification of the rest of the core photograph and other similar core photographs. Hence, data selected for initial classifier training should be representative of the entire well, and chosen carefully so that they contain all the potential classes that need to be identified. Failure to adequately represent all classes will lead to misclassification of the core photograph.

Figure 1 shows an interval of the core photograph used to train and develop the algorithm. It consists of the following lithology classes: carbonate cemented sandstone (9924–9925 ft, 9928.5–9929 ft), shale (9933–9934 ft, 9936–9938 ft), and sandstone (9925–9927 ft). There is also a fourth class which we call 'no-core' containing intervals where either core was missing during coring, or pieces were taken for core analysis and labelled as 'preserved sample'.

[1] *School of Geosciences, University of Edinburgh, Grant Institute, Kings Buildings, Edinburgh EH9 3JW, UK.*
* *A.Thomas-5@sms.ed.ac.uk*

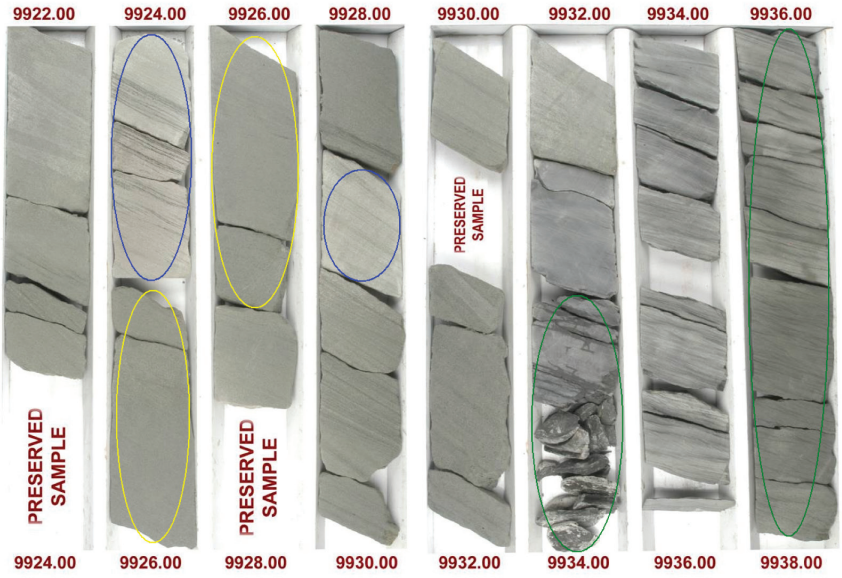

Figure 1 *Core photograph used to develop the protocol for the automated lithology identification. We start with a simple lithology consisting of carbonate-cement (blue circled regions), shale (green), and sandstone (yellow). The white regions in the core photograph are regions where either core was missing during coring, or taken for core analysis and labelled as 'preserved sample'. We add another class called 'no-core' for these regions in the core photograph classification.*

This study is an approach to train the classifier to classify core photographs in a way analogous to how it is carried out using our eyes; hence these distinguishing spectral properties are used to train the classifier to perform an automated lithology extraction. For example, in Figure 1, the dark regions represent shale, light coloured regions represent carbonate cemented sandstone, intermediate coloured regions represent sandy regions, and the white background intervals represent the no-core regions in the core photograph.

Protocol development

Protocols in human communication are separate rules about appearance, speaking, listening, and understanding. They work together to help in successful communication. Similarly, a protocol in object-based image analysis can be defined as a set of rules and controlling parameters that are arranged in a sequential order and work together to automate core photograph classification.

Since a well developed protocol can perform automated core photograph classification on any amount of data, and also on other similar types of core photographs and possibly on core photographs from other wells and fields with minimum effort, all parameters that best classify the core photograph, defined based on the experiments on the core photograph used in this study, are coded as a protocol. A schematic representation of various steps recorded in this protocol, and the experiments involved in finalizing each of these individual steps, are shown in Figure 2.

Image segmentation

This is a process of partitioning an image into non-overlapping regions (Schiewe, 2002). A multi-resolution segmentation algorithm developed by Baatz and Schape (2000) is used for image segmentation, which is a region-merging technique that starts with single-pixel objects. In subsequent iterative steps, adjacent pixels are grouped into larger objects, based on the predefined spectral, $h_{Spectral}$, and shape, h_{Shape}, parameters (defined below), such that these objects define the smallest growth in heterogeneity, f, within each object (Gamanya et al., 2007), where f is defined by

$$f = (1-w)h_{Spectral} + w \cdot h_{Shape} \quad (1)$$

In equation (1), $h_{Spectral}$ is a measure of the object's change in internal heterogeneity resulting from the potential merging of two adjacent objects. Similarly, h_{Shape} is based upon the change in object shape before and after the merge being considered, and w is a weighting parameter, $0 \le w \le 1$, used to define the relative importance of $h_{Spectral}$ and h_{Shape} (Baatz and Schape, 2000). This merging of image objects stops when f exceeds a predefined threshold called the scale parameter, S (Benz et al., 2003) – the maximum allowed change in heterogeneity that may occur when merging objects (Darwish et al., 2003). Appropriate value for S and weights for $h_{Spectral}$ and h_{Shape} are defined by an interactive process until parameters are obtained that best delineate the image objects according to the view of a geologist. Our results show that the best lithology extraction from core photographs were obtained when S and weights for $h_{spectral}$, and h_{shape} were given values of 10, 0.9, and 0.1 (0.5 and 0.5) respectively, but these values may vary depending on the specific field and lithologies or rock types considered.

Knowledge-base design

Object-based image analysis incorporates the power and repeatability of computers with expert human knowledge to classify an image. A knowledge-based scheme (which includes

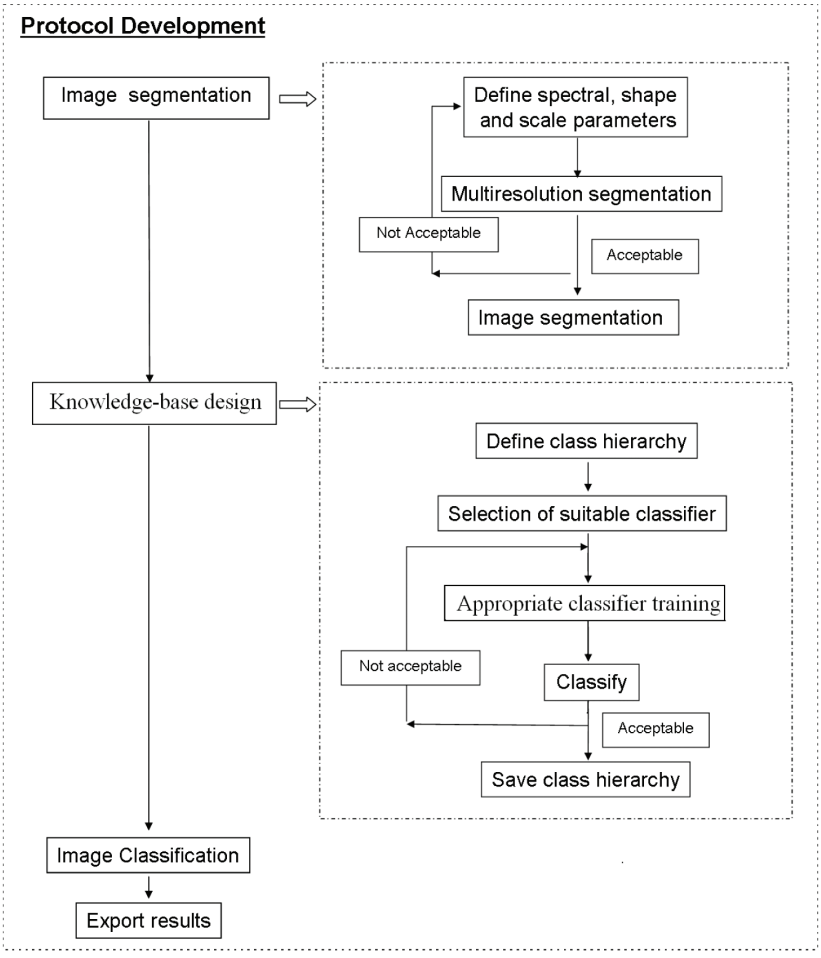

Figure 2 *Schematic representation of various steps recorded in the protocol for automated lithology extraction from core photographs (left) and the experiments involved in finalizing each of these steps (right).*

human interaction) is used to define possible classes present in the core photograph. In this scheme, an expert trains a suitable classification algorithm by selecting representative objects for each class and defining features that could distinguish objects belonging to various classes. The main steps in the knowledge-base design are detailed below.

Defining class hierarchy: Desired classes are named a priori, based on an examination of the core, core data, core photographs, and other geophysical logs. Based on this knowledge, a class hierarchy, which contains all classes in the desired classification scheme, is developed. The defined class hierarchy includes sand, shale, carbonate cements, and no-core regions. The no-core class represents core intervals that are either missing or taken as preserved samples for core analysis.

Defining appropriate image-object features: Segmented objects can be grouped into various classes based on their characteristic features. Hence, various features which can distinguish the segmented objects that belong to different lithology classes are calculated. For example, the mean of the spectral values of all pixels forming each object, their standard deviation, and maxima of the spectral value of each image object are all used in this case.

Selecting and training appropriate classifier: The classification of the image objects is performed by supervised classification, based on fuzzy logic (Benz et al., 2003). All objects in the image are given a value between 0 and 1, which represents the likelihood of their being a member of different classes in the class hierarchy. The classification is carried out using a nearest-neighbour classifier. This is because more than two features were used to distinguish the individual classes present in the core photograph, and nearest-neighbour classifiers can operate in multi-dimensional feature space (Arya, 1994).

In nearest-neighbour classification, the feature range that would represent each class is defined by appropriate sample selection. These samples are selected to represent the entire feature range for each class, summarizing all different heterogeneous appearances of members of the class. The feature ranges defined by these selected samples are used to train the classifier for further classification.

Image classification

Classification is a process of assigning each segmented object to appropriate classes (lithology in this case). The

nearest-neighbour classifier is trained based on the developed knowledge-base and the trained classifier is used for the lithology classification of the entire core photograph.

The principle of image classification is that each object is assigned to a class based on its characteristic features, by comparing it to the predefined feature ranges in the feature space (intuitively, feature space is a cross-plot of all features used). Doing so for all image objects results in the image classification. Hence, once the classes have been defined in the feature space, each image object is compared to the defined feature range of each class, and is assigned to the corresponding class that is closest in the feature space. The distance measure that defines what is meant by 'close' is,

$$d = \sqrt{\sum_f \left(\frac{v_f^{(s)} - v_f^{(o)}}{\sigma_f} \right)^2} \qquad (2)$$

where d is the distance between sample object s and image object o, $v_f^{(s)}$ is the feature value of the sample object for feature f, $v_f^{(o)}$ is the feature value of the image object for feature f, σ_f is the standard deviation of the feature values for feature f within that class. The distance between a sample object and the image object to be classified is thus normalised by the standard deviation of all feature values within that class; hence, a distance value $d = 1$ means that the average distance equals the standard deviation of all features defining a particular class.

The classification result is then compared with the visual interpretation of the core photograph, and is further revised, if need be. Wrongly classified objects, if any, are moved to the correct class either by adding or removing a few sample objects to the training sample sets, to attain the desired classification. Hence, by examining the classification result, the objects selected to train the classifier are further refined and thus we iteratively optimize the (interpreter-derived) knowledge-base that is used for automated core photograph analysis.

The classifier training is refined using the knowledge-base incorporating the expertise of an image interpreter, and is saved as a class hierarchy 'mask' – a library of defined features and distinguishing feature ranges for each class in the class hierarchy, defined and finalized by the above interactive sample selection for each class. The same saved class hierarchy mask can be used to classify similar core photographs. By calling up this class hierarchy mask, the protocol incorporates the knowledge derived from the training areas using the predefined feature space, and thus all segmented objects are compared to these feature ranges in the feature space and are classified accordingly, and automatically. However, this can only be used on similar core photographs as the classes at this point are pre-defined, and hence the features and feature ranges could distinguish these classes only.

The protocol can be adapted in two ways when classifying core photographs from different geological settings:

1) Run the protocol iteratively while editing the class hierarchy mask to correct misclassifications on each iteration to suit the new field.
2) Update the class hierarchy to suit to the new field before running the protocol, and then run the protocol for an automated classification.

In either case the existing class hierarchy can be used as a reference for class arrangement, feature selection, and classifier selection. The rest of the protocol, mainly the segmentation parameters used to generate the image objects by combining adjacent similar pixels together, should work for any field as this part of the process has been optimized by testing on a large number of core photographs (though it could of course be refined further depending on the specific field and lithologies or rock types to be considered).

Results and discussion

Testing the protocol

As a first test of the protocol, the same interval of the core photograph that was used for training the classifier is classified automatically using the protocol. The core photograph has been arranged vertically with depth so that it can be easily compared with other geophysical logs and has been depth-shifted with reference to the image log.

Figure 3 shows the classified core photograph using the protocol plotted against depth. The classified core photograph is shown in the right hand side of the figure, where the yellow colour is sand, green is shale, blue is carbonate cementation, and white regions are where either core was absent or taken as a preserved sample for further core analysis. The grey image left of the classified core photograph is the original core photograph used for the automated classification. Left of the core photograph are the neutron and density logs where yellow shades indicate presence of sand and wide green regions indicate shale. The presence of carbonate cements is not clear from the standard logs. However, the resistivity image, to the left of the calliper and gamma logs, shows fine details of the borehole. The white regions running left to right in the resistivity image logs indicate carbonate cement, which corresponds well to our core photograph interpretation.

Verification of the protocol

The successfully tested protocol is then applied over another interval of the core photograph which was not used for the initial protocol development. Figure 4 shows the classification result on the new interval of the core photograph plotted against depth, along with the original core photograph, resistivity image, and caliper, gamma, neutron, and density logs; the figure key is similar to that of Figure 3.

Accuracy assessment of the result

The classification result is then compared with a qualitative, independent geologist's interpretation based directly on core photographs, which is taken as the ground truth. An accuracy assessment of the automated classification is done by manually selecting samples of each class entirely based on the geologist's interpretation, and comparing them to the automated classification where the objects are assigned automatically into various classes based on the classifier training.

Figure 5 shows the feature space of two features (maximum spectral value of the image objects formed during image segmentation along the x-axis, and the standard deviation of the spectral value of image objects along the y axis). The segmented objects belonging to different classes are plotted based on the geologist's interpretation (big circles), and based on the lithology classes automatically assigned by the classifier (small dots).

A one-to-one comparison of the results is shown in Table 1. Out of the 315 objects 297 classifications are correct in this case, giving an overall accuracy of 94.29%.

Note in particular that there were misclassifications in the regions where a core photograph was absent and had a shadow cast from the existing core pieces. Out of 115 objects assigned into the no-core class based on the geologist's interpretation, a total of 103 were correctly classified into the no-core class by this automated classification, while 12 objects were assigned into carbonate-cement class (Table 1). From the classification result in Figure 4, it is clear that these no-core region misclassifications were due to the shadows cast from the existing core (e.g., can be seen on the classified core photograph at depth interval 9968 ft) and some are due to the improper lighting (can be seen at right and left sides of the classified core photograph intervals 9971–9978 and 9987–9988

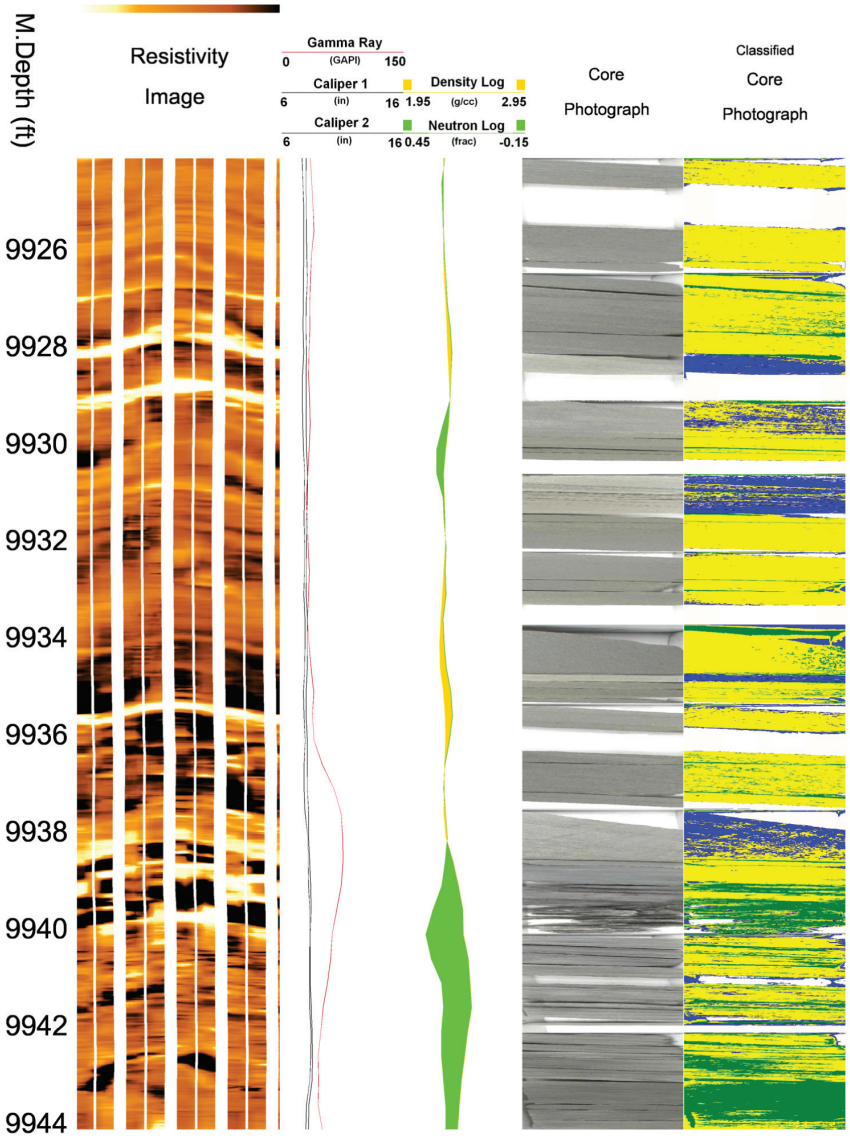

Figure 3 *Core photograph classification result. From left to right, the depth interval, image log, gamma log, and caliper logs, neutron and density logs (most of the yellow shaded region indicates sand and green region shale), core photograph used for this study, and classified core photograph using the object-based image analysis. In the core classification, the yellow regions indicate sand, green shows presence of shale, blue indicates carbonate cements, and white shows no-core regions.*

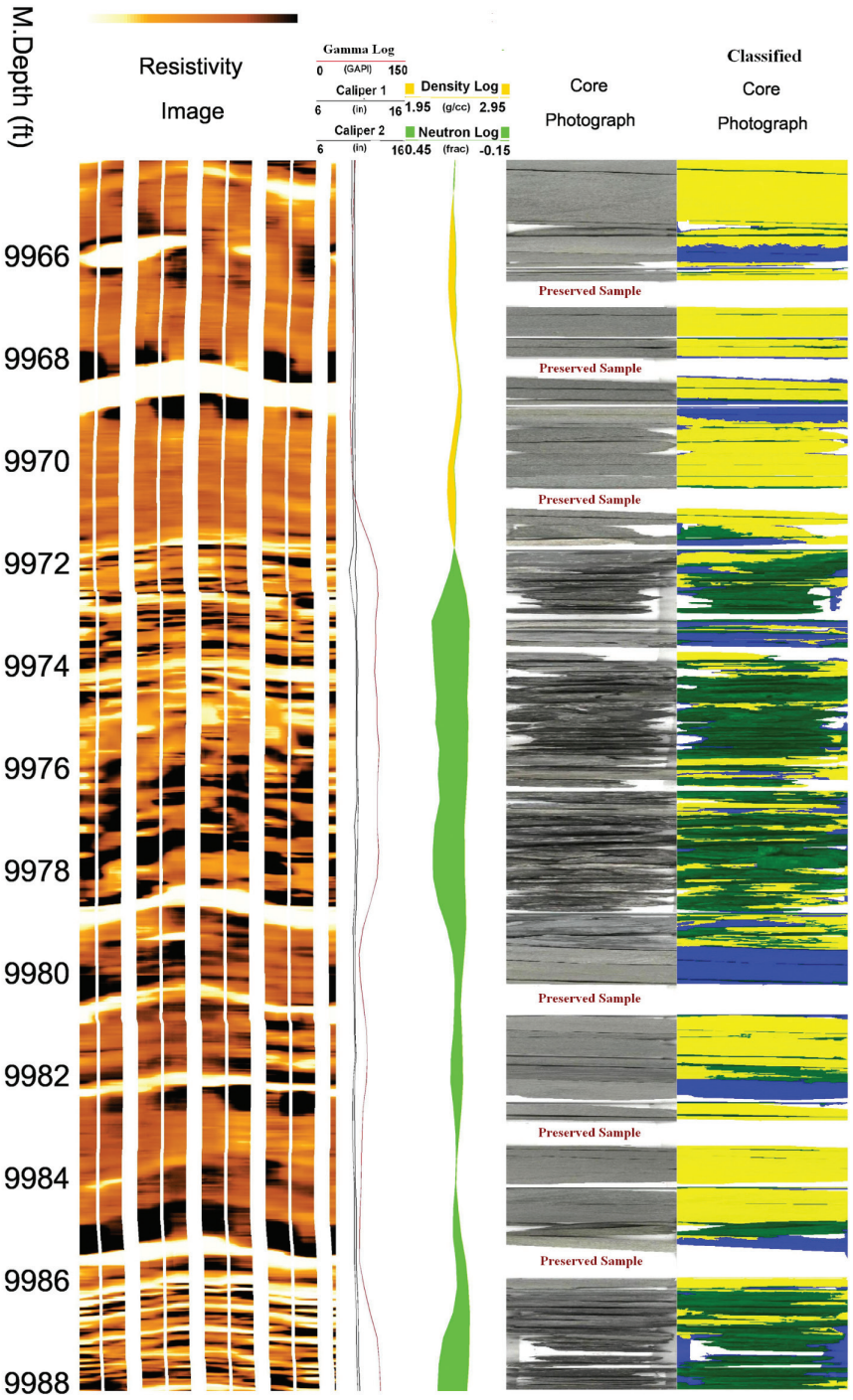

Figure 4 *Testing of the classification protocol: the figure key and colour key are similar to figure 3.*

feet). This is because some of these no-core regions with shadow shared the same spectral values as the carbonate. However, this will not confuse the interpretation of the core photo obtained using this developed protocol, as the human eye can easily distinguish such cases. Ideally, such misclassifications can be removed if the core photographs could be taken against a background of completely different colour to the core, and the lighting was arranged to be directly behind the camera. If this form of misclassification was thus corrected, the overall accuracy would rise to 309/315 = 98%.

Interestingly, the fine variation in lithology at the interval, 9972–9978 feet, has been clearly picked up by this automated classification. Qualitative interpretation of these kinds of fine details can be highly laborious and time-consuming and can be performed only at a very small scale.

	Classification based on samples selected according to geologist's interpretation				
Classification based on automated method		Sand	Shale	Carbonate	No core
	Sand	76	5	0	0
	Shale	1	110	0	0
	Carbonate	0	0	8	12
	No core	0	0	0	103

Table 1 *Accuracy assessment of the classification obtained using the protocol by comparing the automated classification result with the geologist's interpretation. Table shows out of the 315 objects, 297 classifications were correct giving an overall accuracy of 94.29%.*

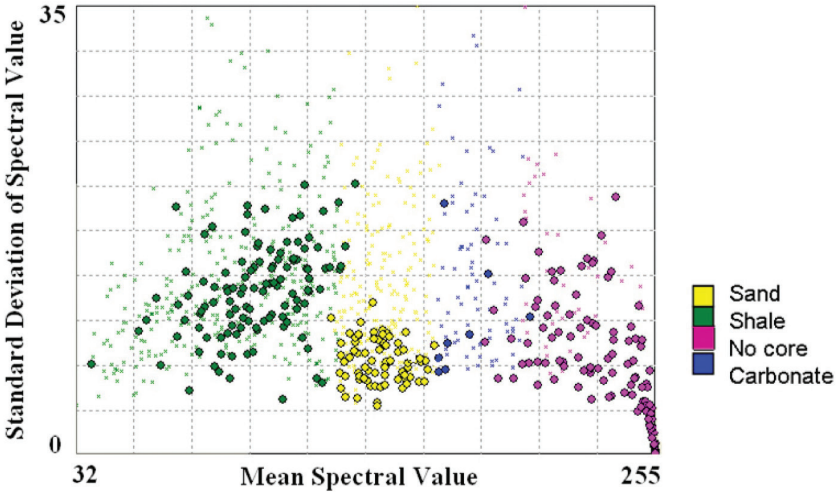

Figure 5 *Space distribution of the object samples – sand (yellow), shale (green), carbonate-cements (blue), and no-core regions (purple). Big dots indicate sample objects based on a geologist's interpretation and small dots represent object classes defined by the protocol.*

Conclusion

An automated method for lithology classification from core photographs using object-based image analysis technology is developed. This method combines both the power of computers and human geological knowledge. A knowledge-based scheme involving human interaction is used to define possible lithology classes present in the core photograph, and to select appropriate samples (objects) which belong to each lithology class. Later a classifier (used for automated classification) is trained to assign all unknown objects into appropriate classes based on this knowledge-base. The methodology can be quickly adapted to core photographs from other geological areas, with adjustments to the knowledge-base used to train the classifier. The automated classification is then calibrated to a geologist's interpretation to ensure the accuracy of the new methodology and the good match between the two gives confidence in this new methodology. This work shows how the object-based image analysis method simplifies the labour intensive visual interpretation of core photographs. Object-based image analysis techniques offer a feasible, robust, and repeatable quantitative extraction of lithology information from core photographs, and offer an efficient and reliable approach to processing large amounts of data. In addition, the methodology is applicable to several kinds of borehole images, for example, wireline electrical borehole images and the more specialized LWD images.

References

Arya, S., Mount, D.M., Netanyahu, N.S. Silverman R. and Wu, A.]1994] An Optimal Algorithm for Approximate Nearest Neighbour Searching. *5th Annual ACM-SIAM Symposium on Discrete Algorithms*, 573–582.

Blackbourn, G. A. [1990] Cores and Core Logging for Geologists. *Whittles Publishing.*

Baatz, M. and Schape, A. [2000] Multiresolution Segmentation - An Optimization Approach for High Quality Multi-Scale Image Segmentation. In: J. Strobl et al. (Eds.) Angewandte Geographische Informationsverarbeitung, XII, *AGIT Symposium*, Salzburg, Germany, 12–23.

Benz, U. C., Hofmann, P. Willhauck, G. , Lingenfelder, I. and Heynen, M. [2004] Multi-Resolution, Object-Oriented Fuzzy Analysis of Remote Sensing Data for GIS-Ready Information. *ISPRS Journal of Photogrammetry & Remote Sensing*, **58**, 239–258.

Darwish, A., Leukert, K.and Reinhart, W. [2003] Image Segmentation for the Purpose of Object-Based Classification. *IGARSS 2003*, IEEE, Toulouse.

Gamanya, R., De Maeyer, P. and De Dapper, M. [2007] An Automated Satellite Image Classification Design Using Object-Oriented Segmentation Algorithms: A Move Towards Standardization. *Expert Systems with Applications,* **32**, 616–624.

Schiewe, J. [2002] Segmentation of High-Resolution Remotely Sensed Data - Concepts, Applications and Problems. *Symposium on Geospatial Theory, Processings and Applications*, Ottawa.